

Catalytic Decomposition of Ammonia over Bimetallic CuO/CeO₂ Nanoparticle Catalyst

Chang-Mao Hung*

Department of Industry Engineering and Management, Yung-Ta Institute of Technology & Commerce,
Pingtung 909, Taiwan, Republic of China

Abstract

The oxidation of ammonia to nitrogen by selective catalytic oxidation (NH₃-SCO) over a bimetallic CuO/CeO₂ nanoparticle catalyst at temperatures between 423 and 673K. A bimetallic CuO/CeO₂ nanoparticle catalyst was prepared by co-precipitation method at molar ratio of 6:4. This study also considers how the concentration of influent NH₃ ($C_0 = 800$ ppm), the space velocity ($GHSV = 92000$ /hr), the relative humidity ($RH = 12\%$) and the concentration of oxygen ($O_2 = 4\%$) affect the operational stability and the capacity for removing NH₃. The catalysts were characterized before and after reaction using EDX, BET, ATR-FTIR, PSA and TEM. The catalytic performance show that the ammonia was removed by oxidation in the presence of bimetallic CuO/CeO₂ nanoparticle catalyst, and around 98% at complete NH₃ reduction was achieved, and a high selectivity toward N₂ during catalytic oxidation over the catalyst at 673K with an oxygen content of 4.0%. Moreover, the effect of the reaction temperature on the removal of NH₃ in the gaseous phase was also monitored at a gas hourly space velocity of under 92000/hr.

Keywords: Selective catalytic oxidation (SCO); Tubular fixed-bed reactor (TFBR); Ammonia; Bimetallic CuO/CeO₂ nanoparticle catalyst.

INTRODUCTION

Nowadays, ammonia (NH₃) is used in the ammonium nitrate and nitric acid production industry, livestock feedlots, urea manufacturing plants, the nitrogen fertilizer

application industry, fossil fuel combustion and petroleum refineries as well as the refrigeration industry (Ng *et al.*, 2007; Chou *et al.*, 2007; Xu *et al.*, 2008). As is known, ammonia is a toxic inorganic gas with a pungent odor under ambient conditions, and is potentially harmful to public health (Geng *et al.*, 2008; Lin *et al.*, 2008). Conventional biological, physical and chemical treatments, including biofilters, stripping, scrubbing with

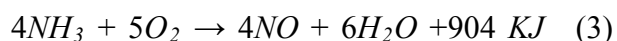
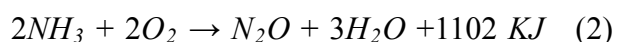
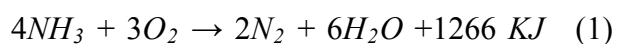
*Corresponding author: TEL: +886-8 723-3733 ext 508;

Fax: +886-8722-8046

E-mail address: hungcm1031@gmail.com

water, post-combustion control, microwave-plasma discharge, electrochemical oxidation and the use of activated carbon fibers for soot adsorption, only trigger a phase transformation and may yield a contaminated sludge and/or an adsorbent, both of which require further treatment. The maintenance and operating costs associated with these physical and/or chemical methods are high. Therefore, the removal and the control and prevention, of the emission of ammonia emission from air and waste streams are important due to environmental concerns.

More recently, catalytic oxidation has been established to increase the effectiveness of advanced oxidation processes technology using dedicated catalysts, which potentially shorten the reaction times of oxidation, and allow it to proceed under milder operating conditions. The selective catalytic oxidation of ammonia (NH₃-SCO) in a stream to molecular nitrogen and water is one method for solving problems of ammonia pollution (Dravell *et al.*, 2003). The catalytic oxidation of ammonia has been reported to precede as follows the exothermic global reactions:



The SCO process that involves ammonia should be selective for nitrogen (reaction 1), and prevent further oxidation of nitrogen (reactions 2 and 3). Earlier work on ammonia

oxidation was reviewed by Il'chenko (1976), who focused on the reaction mechanism of ammonia oxidation, and compared catalytic activities. Few catalysts have been used in oxidizing ammonia in the gaseous phase. For instance, Wang *et al.* (1999), who developed Ni-based catalysts for oxidizing fuel gas generated by gasifying biomass, found that fresh Ni-based catalysts were more active at lower temperatures in decomposing ammonia, and the partial pressure of hydrogen in the flue gas is a critical factor that governed ammonia oxidation. Moreover, Liang (2000) studied the oxidation of ammonia in a fixed-bed microreactor in the temperature range 873-1023K at GHSV=1800-3600/hr. They found that the conversion of ammonia reached 98.7% and 99.8% on nitrated MoN_x/α-Al₂O₃ and NiMoNy/α-Al₂O₃ catalysts, respectively. Schmidt-Szałowski (1998) also developed a hypothetical model of the effect of these catalysts and their activity and selectivity in oxidizing ammonia. Recently, Pansare and Jr. Goodwin (2008) summarized the catalytic oxidation of ammonia in the presence of synthesis gas produced from biomass gasification by tungsten-based catalyst in the temperature range 738-923K. There is a significant effect of the catalyst calcinations temperature, which is the material with the highest ammonia reduction activity.

Copper and cerium metals with fluorite-type oxides have been used to elucidate the reduction characteristics of methane conversion (Kundakovic *et al.*, 1998). The interaction between copper and the cerium is complex, because various Cu-Ce

interactions can result in synergistic effects and oxygen vacancies, enhancing catalytic characteristics (Skårman *et al.*, 2002; Hung, 2006). However, little work has been undertaken on the use of Cu-Ce composite metal catalyst to determine the reactive characteristics of these active metals in catalytic oxidation. Due to these properties, the activity of the bimetallic CuO/CeO₂ nanoparticle catalyst in the oxidation of ammonia given various values of parameters and its effect on the removal of ammonia in selective catalytic oxidation processes (NH₃-SCO) were studied. For these purpose, different techniques approach using EDX, BET, ATR-FTIR, PSA and TEM were employed to examine the behavior of bimetallic CuO/CeO₂ nanoparticle catalyst.

MATERIALS AND METHODS

Preparing bimetallic CuO/CeO₂ nanoparticle catalyst

Bimetallic CuO/CeO₂ nanoparticle catalyst used in this work were prepared by the by the co-precipitation of copper (II) nitrate (GR grade, Merck, Darmstadt, Germany) and cerium (III) nitrate (GR grade, Merck, Darmstadt, Germany) at molar ratio of 6:4. The composite catalysts were then calcined at 773K in an airstream for four hours. The resulting powder was made into tablets using acetic acid as a binder. The tablets were later reheated at 573K to burn the binder out of the CuO/CeO₂ composite tablets. The tablets were then crushed and sieved into various particle sizes ranging from 0.25-0.15 mm for use later.

Characterizing the solid phase

The composition of the catalyst's surface was determined using an energy-dispersive x-ray spectrometer (SEM/EDX, JEOL, JSM-6400, Kevex, DeltaII). The amount of carbonaceous deposit on the used bimetallic CuO/CeO₂ nanoparticle catalyst surface was determined by carbon-hydrogen-nitrogen elemental analysis (Carlo Erba, model EA 1108, Milan, Italy). The specific surface areas of the composite catalysts were determined by the physical adsorption of nitrogen at 77K using a Brunauer, Emmett, and Teller model and a BET surface area analyzer (ASAP 2000, Micromeritics, Norcross, Georgia). Diffuse reflectance ATR-FTIR spectra of species adsorbed on the catalyst were measured at room temperature using a Bruker Vector 22 FTIR spectrometer, equipped with a diffuse reflectance attachment with a resolution of 4/cm (Bruker, Germany). The changes in the sizes of the catalytic particles were measured using a laser light-scattering particle size analyzer (PSA, Coulter LS100, USA). Transmission electron microscopy (TEM) (Philips CM-200 Twin, Netherlands) elucidated the morphology of the catalysts and yielded information on the distribution of copper-cerium species on the catalyst surface.

Catalytic tests

Experiments were conducted on a tubular fixed-bed flow quartz reactor (TFBR). Two flowing gases, NH₃ and O₂, were used to prepare the feed mixture in the diluting gas, helium, which flowed into the inlet of the reactor. A mass flow regulator was used to

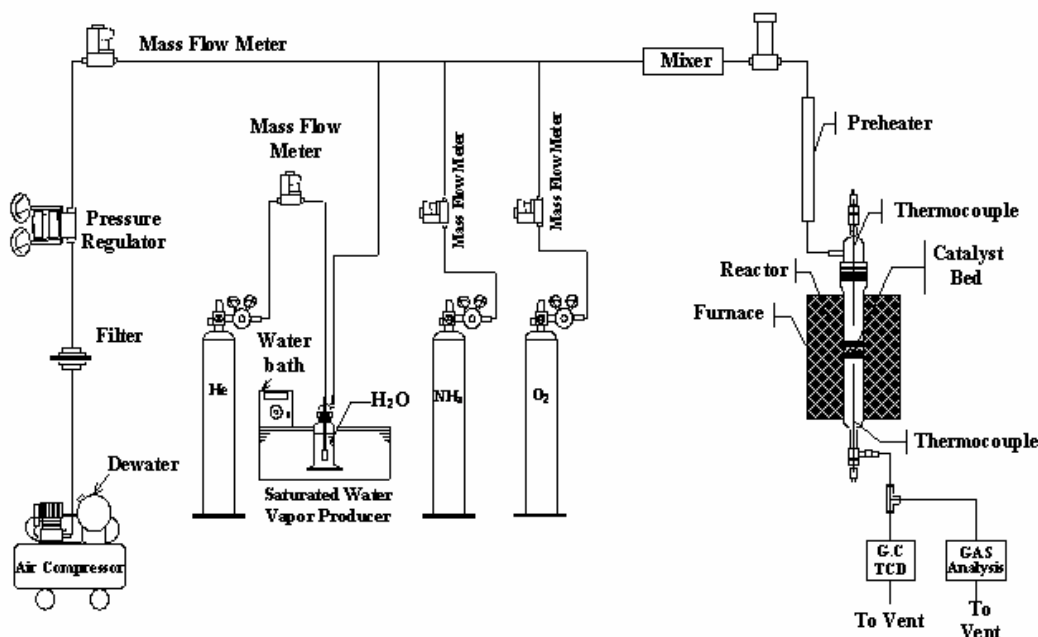


Fig. 1. Schematic diagram of the tubular fixed-bed reaction (TFBR) system.

control independently the flows of ammonia and oxygen. Extremely pure helium was used as a carrier gas at a flow rate from 8-13 L/min, controlled using a mass flow meter (830 Series Side-Trak™, Sierra, Monterey, CA, USA). The mass of each catalyst was 1 g and the empty bed volume was approximately 1.2 cm³. An inert material formed from (hydrophilic and inert) γ -Al₂O₃ spheres was used to increase the interfacial area between the solid and the gas phase to increase the mass transfer of ammonia from gaseous streams. This approach resembled that of Hung *et al.* (2008), who conducted experiments on the catalytic oxidation of ammonia. A reaction tube with a length of 300 mm and an inner diameter of 28-mm was placed inside a split tube furnace. The tube that contained the catalyst was placed in the same furnace. The temperature was measured using two type-K thermocouples (KT-110, Kirter, Kaohsiung, Taiwan), each with a

diameter of 0.5 mm, these were located in front of and behind the catalytic bed. The thermocouples were also connected to a PID controller (FP21, Shimaen, Tokyo, Japan) to maintain the temperature in the tube within $\pm 0.5\%$. The concentration of the feed gas (GHSV, 92000 mL/h-g) was maintained at 1000 ppm NH₃ and the O₂ concentration was 4%. The catalyst was not deactivated during testing. Fig. 1 schematically depicts the tubular fixed-bed reaction system (TFBR).

Catalytic performance measurement

Before and after the reaction, samples were automatically injected through a sampling valve into a gas chromatograph (Shimadzu GC-14A), equipped with a thermal conductivity detector. A stainless-steel column (Porapak Q 80/100mesh) was used to separate and determine the concentrations of N₂O isothermally at 373K. The areas associated with the signals were electronically measured

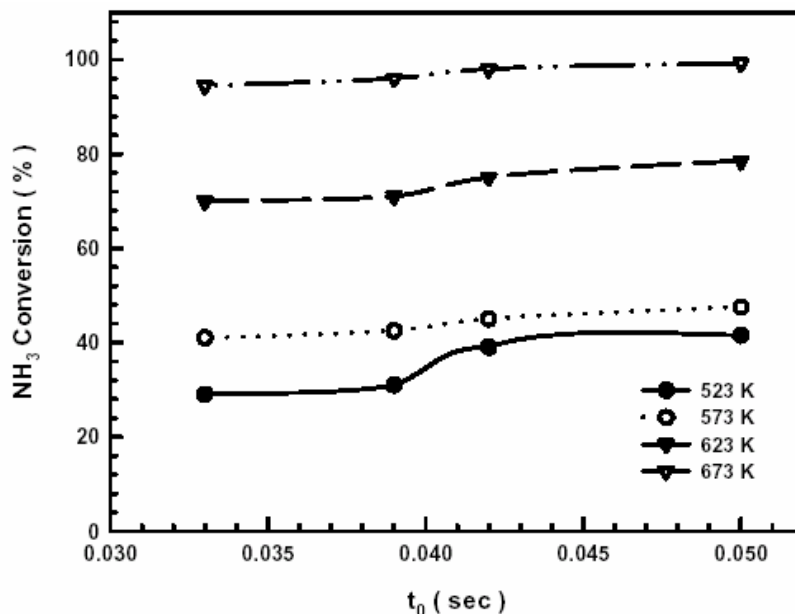


Fig. 2. Effect of empty bed residence time (EBRT) on the bimetallic CuO/CeO₂ nanoparticle catalyst for the conversion of NH₃ as function of temperature. Test conditions: 800 ppm NH₃ in He, O₂ = 4%, GHSV = 92000 mL/h-g.

using a data integrator (CR-6A, Shimadzu, Kyoto, Japan). Dilute sulfuric acid was used to scrub the residual ammonia in the vapor gas and the amount present was measured using a Merck kit (Merck, Spectroquant Vega 400, Darmstadt, Germany). The concentrations of NO, NO₂ and O₂ in the gas samples were monitored continuously during combustion at a particular location, using a portable flue gas analyzer (IMR-3000, Neckarsulm, Germany). Data were collected when the SCO reaction was in a steady state, typically after 20 min at each temperature. Each temperature was maintained for 90 min to allow the system to enter a steady state. Most experiments were repeated once to ensure reproducibility, and similar results were always obtained.

RESULTS AND DISCUSSION

Fig. 2 plots the effect on the reduction of NH₃ of the bimetallic CuO/CeO₂ nanoparticle catalyst used in the oxidation of NH₃ stream, in terms of the reaction temperature and the empty bed residence time (EBRT) of the influent stream. The results indicate that increasing the EBRT increased the efficiency of oxidation of NH₃. Increasing the reaction temperature was also observed to increase the extent of NH₃ oxidation. When the EBRT of the influent stream was set to 0.05 sec, about 98.0% of the NH₃ was reduced at 673K in the catalytic run, whereas only a 38.0% of NH₃ was removed using the catalysis at 523K. Normally, the amount of NH₃ removed by the catalyzed reaction was observed to be around 98.0% greater than that observed to be removed by the SCO process runs at 673K at a EBRT of under 0.05 sec.

With reference to the composition of copper

Table 1. Surface composition analysis of the test catalyst.

Element percentage (%)	6:4 ^a	6:4 ^b
Cu ^c	61.12	58.52
Ce ^c	38.82	35.01
C ^d	0.32	0.29
H ^d	0.35	0.33
O ^d	10.36	10.70
N ^d	0	0

^a New catalyst.

^b Used catalyst after 72 hours in fixed bed oxidation reactor.

^c Determined by EDX.

^d Determined by carbon-hydrogen-nitrogen elemental analysis.

and cerium from the catalyst, as presented in Table 1, analysis of the elemental composition of the surfaces of the test catalysts reveals that the composition of metal ions from the bimetallic CuO/CeO₂ nanoparticle catalyst varied slightly. The element oxygen percentage increasing in the catalyst surface, as shown in Table 1, is due to the oxygen ions conducted by CeO₂, in which the structure has a synergistic Cu-O_{vacancy} interaction sites in nanoparticles (Sasi *et al.*, 2003). In greater detail, the oxygen that oxidizes ammonia over the bimetallic CuO/CeO₂ nanoparticle catalyst is present in the lattice structure of the catalyst (as β oxygen) and as adsorbed oxygen (α oxygen). α oxygen is related to the oxygen vacancy of catalyst surface: α oxygen content increases with the number of oxygen vacancies (Sedmak *et al.*, 2003).

The adsorptive and catalytic behavior of a catalyst is strongly influenced by the capacity and texture of its exterior surface. Fig. 3. summarizes the properties of test catalysts determined by BET (Brunauer-Emmett-Teller method) analysis, including specific surface

area. The specific surface area was 60 m²/g at 523K. At the 673K on a bimetallic CuO/CeO₂ nanoparticle catalyst, the surface areas slightly decreased (43 m²/g). This test showed that the catalysts were associated with a larger lattice surface of copper or cerium, and that higher temperature caused metal sintering, perhaps reducing catalytic activity. Clearly, reaction temperature conditions are important role in activating the generated surface, and the increase in surface area may not be the main factor in that promotes the activity.

The overall selectivity of N₂ production varied from 19-85% and that of NO production varied from 0-4% over the range of 11.0-98.0% NH₃ conversion at NH₃ concentrations of 800 ppm (Fig. 4). Nitrogen gas thought to be formed primarily by the dissociation of NO produced by oxidation of adsorbed NH₃ (Bradley *et al.*, 1995). Therefore, we hypothesis that NH₃ and oxygen may be adsorbed onto specific sites on the bimetallic CuO/CeO₂ nanoparticle catalyst, promoting the rapid conversion of NH₃ to nitrogen and water. Nitrogen was the

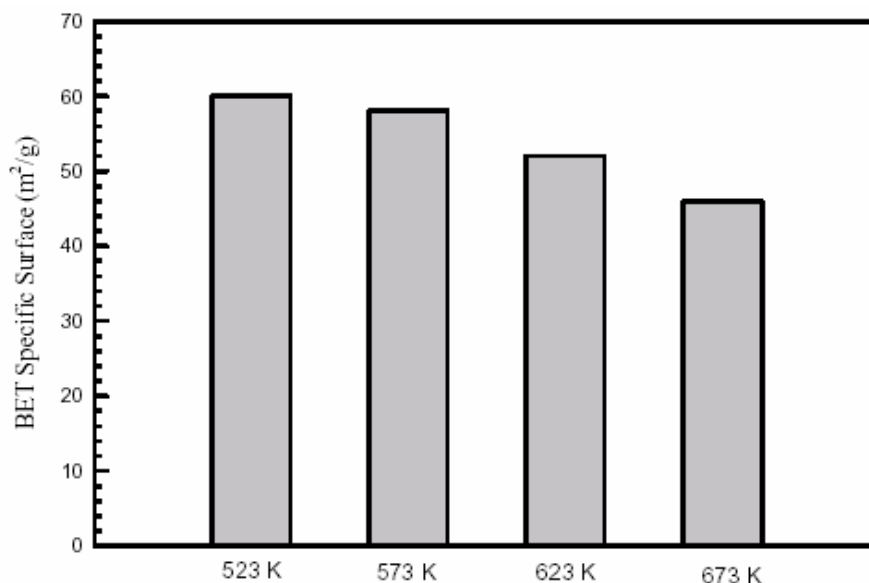


Fig. 3. Effect of reaction temperature with changes of specific surface area on the bimetallic CuO/CeO₂ nanoparticle catalyst for the conversion of NH₃. Test conditions: 800 ppm NH₃ in He, O₂ = 4%, RH = 18%, GHSV = 92000 mL/h-g.

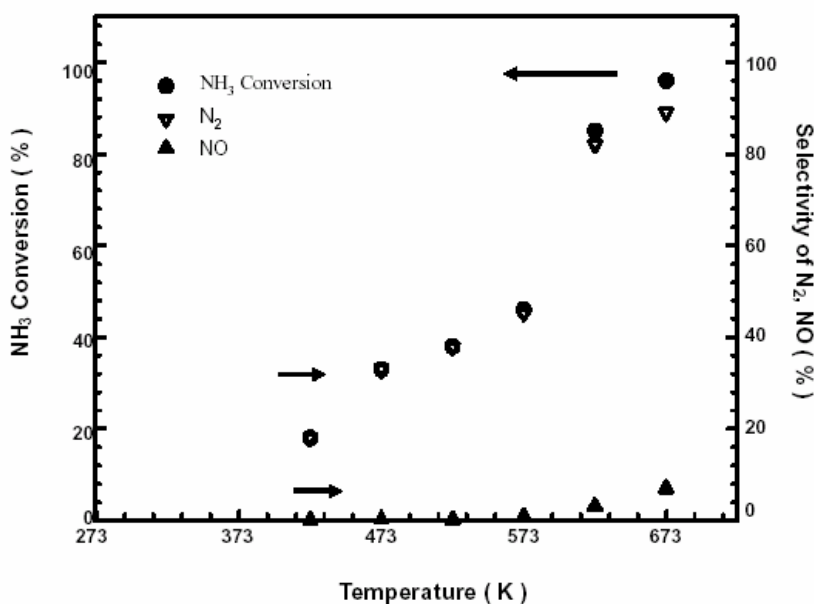


Fig. 4. Relationship of the ammonia conversion, N₂ yield, and NO yield at various temperatures over the bimetallic CuO/CeO₂ nanoparticle catalyst. Test conditions: 800 ppm NH₃ in He, O₂ = 4%, RH = 12%, Temp = 423-673K, GHSV = 92000 mL/h-g.

dominant gaseous, and a small amount of NO was detected in the resultant stream. This

result is similar to that obtained by Curtin *et al.* (2000).

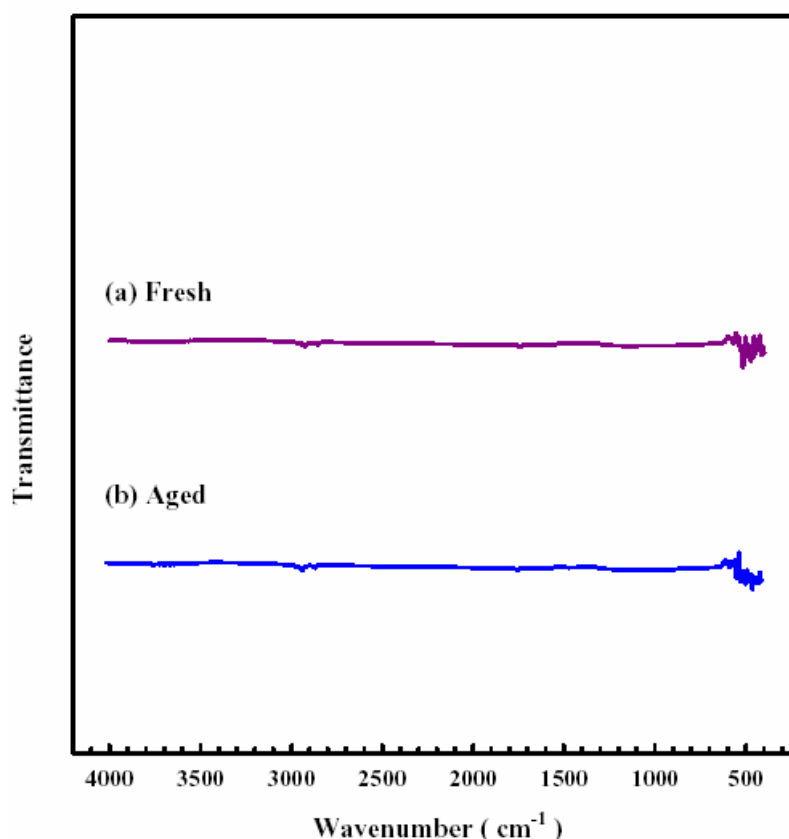


Fig. 5. ATR-FTIR pattern of the bimetallic CuO/CeO₂ nanoparticle catalyst. (a) fresh, (b) after activity test. Test conditions: 800 ppm NH₃ in He, O₂ = 4%, GHSV = 92000 mL/h-g.

Fig. 5. compares the ATR-FTIR spectra of fresh and used catalysts, also verifying the presence of the CuO-like phase 510 cm⁻¹ of the catalyst (Sadykov *et al.*, 2001). As illustrated in Fig. 5, the monodentate nitrite, nitro group anions and hydroxyl groups on the framework are associated with a peak at about 2990 cm⁻¹ and 2820 cm⁻¹ for used catalysts (Blanco *et al.*, 1993).

The change in the sizes of particles of the catalyst was determined using the laser light-scattering method, as depicted in Fig. 6. The mean particle size converged to approximately 15.9 μm for fresh bimetallic

CuO/CeO₂ nanoparticle catalyst. However, the diameters of the catalyst declined after activity test and the mean particle size was around 13.3 μm, indicating that co-precipitation aggregates the high reaction temperature. Hence, such changes in the sizes of particles of the catalyst can be attributed to over-oxidation of the bimetallic CuO/CeO₂ nanoparticle catalyst surface during the reaction.

Fig. 7. presents the surface morphological changes of bimetallic CuO/CeO₂ nanoparticle catalyst elucidating using TEM to provide information on the fresh/aged catalyst surface

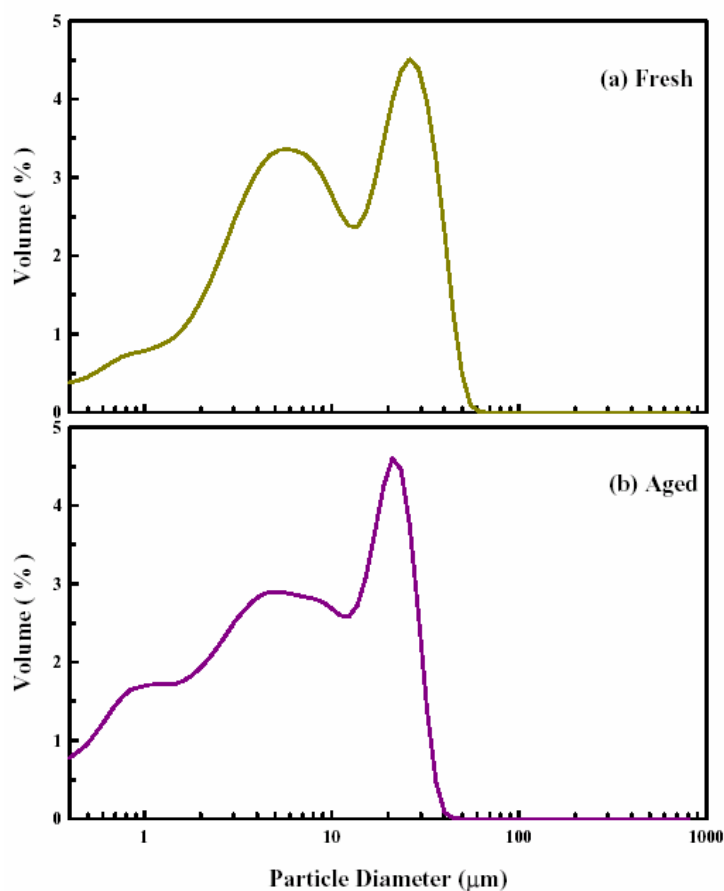


Fig. 6. Changes in particle sizes distribution of the bimetallic CuO/CeO₂ nanoparticle catalyst. (a) fresh, (b) after activity test. Test conditions: 800 ppm NH₃ in He, O₂ = 4%, GHSV = 92000 mL/h-g.

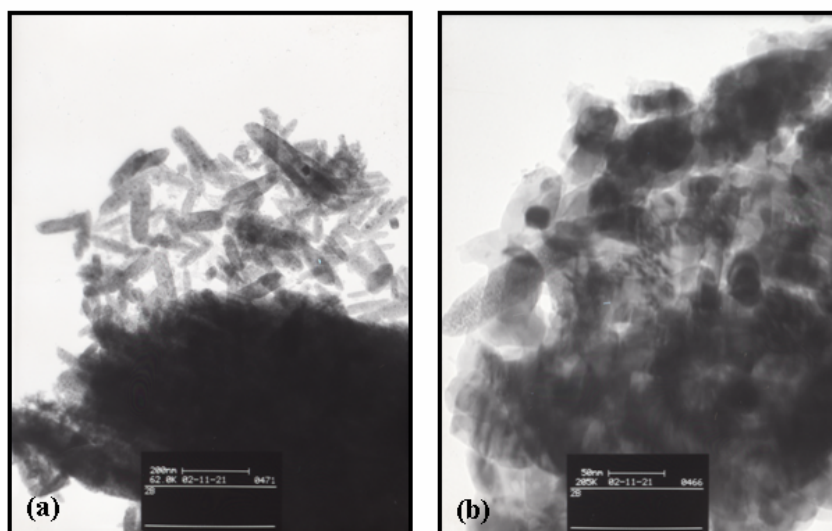


Fig. 7. TEM photograph of (a) fresh and (b) after activity test bimetallic CuO/CeO₂ nanoparticle catalyst. Test conditions: 800 ppm NH₃ in He, O₂ = 4%, GHSV = 92000 mL/h-g.

structure. Fig. 7a. indicates that bimetallic CuO/CeO₂ nanoparticle catalyst exhibits more aggregation and crystalline than observed in Fig. 7b. These crystallinity phases may explain the high activity of the catalysts. Fig. 7b. indicates that disaggregated phases were formed when the surface of the catalyst was aged or when poisoning occurred because of plugging, implying that the porosity of the particles had changed. Based on the above results, it also can be confirmed that the dispersion phenomena of the bimetallic CuO/CeO₂ nanoparticle catalyst increase the efficiency of removal of NH₃.

CONCLUSIONS

The present study has shown that selective catalytic oxidation for ammonia (NH₃-SCO) by a bimetallic CuO/CeO₂ nanoparticle catalyst was found to promote the oxidation of NH₃. The SCO process was found to be more effective at lower temperatures. The process altered the oxidation state and the crystalline composition of the catalyst. The overall by-product selectivity of the production of NO varied from 0-4% and that of N₂ production varied from 19-85% at 20.0-98.0% NH₃ conversion, when a bimetallic CuO/CeO₂ nanoparticle catalyst was used. Also, changes in oxidation state and the crystalline composition of the catalyst were identified. This work shows that the SCO process has the potential to treat highly concentrated streams of NH₃, helping industrial plants to meet discharge regulations.

ACKNOWLEDGMENTS

The authors would like to thank the National Science Council of the Republic of China, Taiwan for partially financially supporting this research under Contract Number NSC 97-2221-E-132-003.

REFERENCES

- Blanco, J., Avila, P. and Fierro, J.L.G. (1993). Influence of Nitrogen Dioxide on the Selective Reduction of NO_x with a Catalyst of Copper and Nickel Oxides. *Appl. Catal. A* 96: 331-343.
- Bradely, J.M., Hopkinson, A. and King, D.A. (1995). Control of a Biphase Surface Reaction by Oxygen Coverage: the Catalytic Oxidation of Ammonia over Pt {100}. *J. Phys. Chem.* 99: 17032-17042.
- Chou, M.S. and Wang, C.H. (2007). Treatment of Ammonia in Air Stream by Biotrickling Filter. *Aerosol Air Qual. Res.* 7: 17-32.
- Curtin, T., Regan, F.O., Deconinck, C., Knüttle, N. and Hodnett, B.K. (2000). The Catalytic Oxidation of Ammonia: Influence of Water and Sulfur on Selectivity to Nitrogen over Promoted Copper Oxide/Alumina Catalysts. *Catal. Today* 55: 189-195.
- Dravell, L.I., Heiskanen, K., Jones, J.M., Ross, A.B., Simell, P. and Williams, A. (2003). An Investigation of Alumina-Supported Catalysts for the Selective Catalytic Oxidation of Ammonia in Biomass Gasification. *Catal. Today* 81: 681-692.
- Geng, Q., Guo, Q., Cao, C., Zhang, Y. and

- Wang, L. (2008). Investigation into Photocatalytic Degradation of Gaseous Ammonia in CPR. *Ind. Eng. Chem. Res.* 47, 4363-4368.
- Hung, C.M. (2006). Selective Catalytic Oxidation of Ammonia to Nitrogen on CuO-CeO₂ Bimetallic Oxide Catalysts. *Aerosol Air Qual. Res.* 6: 150-169.
- Hung, C.M. (2008). Decomposition Kinetics of Ammonia in Gaseous Stream by a Nanoscale Copper-Cerium Bimetallic Catalyst. *J. Haz. Mat.* 150: 53-61.
- Il'chenko, N.I. (1976). Catalytic Oxidation of Ammonia. *Russ. Chem. Rev.* 45: 1119-1134.
- Kundakovic, L. and Flytzani-Stephanopoulos, M. (1998). Reduction Characteristics of Copper Oxide in Cerium and Zirconium Oxide Systems. *Appl. Catal. A: Gen.* 171: 13-29.
- Liang, C., Li, W., Wei, Z., Xin, Q. and Li, C. (2000). Catalytic Decomposition of Ammonia over Nitrided MoN_x/α-Al₂O₃ and NiMoNy/α-Al₂O₃ Catalysts. *Ind. Eng. Chem. Res.* 39: 3694-3697.
- Lin, C.H., Wu, Y.L., Lai, C.H., Watson, J.G. and Chow, J.C. (2008). Air Quality Measurements from the Southern Particulate Matter Supersite in Taiwan. *Aerosol Air Qual. Res.* 8: 233-264.
- Ng, P.F., Li, L., Wang, S., Zhu, Z., Lu, G. and Yan, Z. (2007). Catalytic Ammonia Decomposition over Industrial-Waste-Supported Ru Catalysts. *Environ. Sci. Technol.* 41: 3758-3762.
- Pansare, S.S. and Jr. Goodwin, J.G. (2008). Ammonia Decomposition on Tungsten-Based Catalysts in the Absence and Presence of Syngas. *Ind. Eng. Chem. Res.* 47: 4063-4070.
- Sadykov, V.A., Bunina, R.V., Alikina, G.M., Ivanova, A.S., Kochubei, D.I., Novgorodov, B.N., Paukshtis, E.A., Felonov, V.B., Zaikovskii, V.I. and Kuznetsova, T.G. (2001). Supported CuO + Ag/partially Stabilized Zirconia Catalysts for the Selective Catalytic Reduction of NO_x under Lean Burn Conditions : 1. Bulk and Surface Properties of the Catalysts. *J. Catal.* 200: 117-130.
- Sasi, F., Duprez, D., Gérard, F. and Miloudi, A. (2003). Hydrogen Formation in the Reaction of Steam with Rh/CeO₂ Catalyst: a Tool for Characterizing Reduced Centers of Ceria. *J. Catal.* 213: 226-234.
- Schmidt-Szałowski, K., Krawczyk, K. and Petryk, J. (1998). The Properties of Cobalt Oxide Catalyst for Ammonia Oxidation. *Appl. Catal. A: Gen.* 175: 147-157.
- Sedmak, G., Hočevár, S. and Levec, J. (2003). Kinetics of Selective CO Oxidation in Excess of H₂ over the Nanostructured Cu_{0.1}Ce_{0.9}O_{2-y} Catalyst. *J. Catal.* 213: 135-150.
- Skårman, B., Grandjean, D., Benfield, R.E., Hinz, A., Andersson, A. and Wallenberg, L.R. (2002). Carbon Monoxide Oxidation on Nanostructured CuO_x/CeO₂ Composite Particles Characterized by HREM, XPS, XAS, and High-Energy Diffraction. *J. Catal.* 211: 119-133.
- Wang, W., Padban, N., Ye, Z., Andersson, A. and Bjerle, I. (1999). Kinetic of Ammonia Decomposition in Hot Gas Cleaning. *Ind.*

Eng. Chem. Res. 38: 4175-418.

Xu, X., Barsha, N. and Li, J. (2008).
Analyzing Regional Influence of Particulate
Matter on the City of Beijing, China.

Aerosol Air Qual. Res. 8: 78-93.

Received for review, July 18, 2008

Accepted, August 26, 2008